CHEMISTRY OF MATERIALS
Article

Chem. Mater. **2010,** *22,* 949–956 949
DOI:10.1021/cm901819c

Interfacial Observation between $LiCoO_2$ Electrode and $Li_2S-P_2S_5$ Solid Electrolytes of All-Solid-State Lithium Secondary Batteries Using Transmission Electron Microscopy†

Atsushi Sakuda, Akitoshi Hayashi,* and Masahiro Tatsumisago

Department of Applied Chemistry, Graduate School of Engineering, Osaka Prefecture University, 1-1, Gakuen-cho, Naka-ku, Sakai, Osaka 599-8531, Japan

Received June 26, 2009. Revised Manuscript Received September 8, 2009

In all-solid-state lithium secondary batteries, both the electrode and electrolyte materials are solid. The electrode and solid electrolyte interface's structure and morphology affect a battery's electrochemical performance. Observation of the interface between $LiCoO_2$ positive electrode and highly lithium-ion-conducting $Li_2S-P_2S_5$ solid electrolyte was conducted using transmission electron microscopy. An interfacial layer was formed at the interface between $LiCoO_2$ electrode and $Li_2S-P_2S_5$ solid electrolyte after the battery's initial charge. Furthermore, mutual diffusions of Co, P, and S at the interface between $LiCoO_2$ and $Li_2S-P_2S_5$ were observed. The mutual diffusion and the formation of the interfacial layer were suppressed using $LiCoO_2$ particles coated with Li_2SiO_3 thin film. Results showed that all-solid-state cells using Li_2SiO_3-coated $LiCoO_2$ had better electrochemical performance than those using noncoated $LiCoO_2$. The all-solid-state cells functioned at −30 °C. Moreover, the all-solid-state cell using Li_2SiO_3-coated $LiCoO_2$ was charged and discharged under a high current density of 40 mA cm^{-2} at 100 °C.

Introduction

Lithium ion secondary batteries offer large energy densities. They have been used as power sources of various portable devices.[1] Commercially produced lithium ion secondary batteries consist mainly of $LiCoO_2$ as a positive electrode, carbon as a negative electrode, and an organic electrolyte solution. As an effective approach to improve the batteries' electrochemical performance, interfacial modifications between the positive electrode and electrolyte by coatings of Al_2O_3, ZrO_2, SiO_2, $AlPO_4$, and AlF_3 on the $LiCoO_2$ positive electrode have been studied.[2−7] That modification efficiently improves the batteries' cycle performance, rate capability, and thermal stability. The effects of the modification are (i) suppression of structural change caused by phase transition of $LiCoO_2$, (ii) decrease of cobalt dissolution from $LiCoO_2$ to liquid electrolyte, and (iii) suppression of side reactions between the electrode and electrolyte.

For application to electric vehicles (EV) and hybrid electric vehicles (HEV), development of large-scale lithium secondary batteries with high safety has been strongly desired. Conventional lithium ion secondary batteries entail risks of fire or explosion because of the use of flammable organic electrolyte solutions. From the perspective of safety, all-solid-state batteries using inorganic solid electrolytes represent a superior battery.[8] To construct high-performance all-solid-state batteries, highly lithium-ion-conducting solid electrolytes are required. Sulfide-based solid electrolytes show remarkably high lithium-ion conductivity.[9−11] Among them, $Li_2S-P_2S_5$ glass ceramics show high lithium-ion conductivity of more than 1×10^{-3} S cm^{-1} at room temperature, along with a wide electrochemical window over 5 V.[11,12] We reported that the all-solid-state batteries using $LiCoO_2$ electrode and $80Li_2S \cdot 20P_2S_5$ (mol %) glass-ceramic solid electrolyte exhibited long cycle performance.[13] However, all-solid-state batteries have generally been difficult to operate at high current densities of more than several milliamperes

† Accepted as part of the 2010 "Materials Chemistry of Energy Conversion Special Issue".

*Corresponding author. Tel.: +81−72−254−9334. Fax: +81−72−9334. E−mail: hayashi@chem.osakafu-u.ac.jp.

(1) Tarascon, J.-M.; Armand, M. *Nature* **2001**, *414*, 359–367.
(2) Cho, J.; Kim, Y.-J.; Park, B. *Chem. Mater.* **2000**, *12*, 3788–3791.
(3) Cho, J.; Kim, Y. J.; Kim, J.-T.; Park, B. *Angew. Chem., Int. Ed.* **2001**, *40*, 3367–3369.
(4) Cho, J.; Kim, B.; Lee, J.-G.; Kim, Y.-W.; Park, B. *J. Electrochem. Soc.* **2005**, *152*, A32–A36.
(5) Chen, Z.; Dahn, J. R. *Electrochem. Solid-State Lett.* **2003**, *6*, A221–A224.
(6) Chen, Z.; Dahn, J. R. *Electrochim. Acta* **2004**, *49*, 1079–1090.
(7) Sun, Y.-K.; Cho, S.-W.; Myung, S.−T.; Amine, K.; Prakash, J. *Electrochim. Acta* **2007**, *53*, 1013–1019.
(8) Minami, T. *Solid State Ionics for Batteries*; Springer-Verlag: Tokyo, 2005.
(9) Kanno, R.; Murayama, M. *J. Electrochem. Soc.* **2001**, *148*, A742–A746.
(10) Hayashi, A.; Hama, S.; Minami, T.; Tatsumisago, M. *Electrochem. Commun.* **2003**, *5*, 111–114.
(11) Mizuno, F.; Hayashi, A.; Tadanaga, K.; Tatsumisago, M. *Adv. Mater.* **2005**, *17*, 918–921.
(12) Hayashi, A.; Hama, S.; Mizuno, F.; Tadanaga, K.; Minami, T.; Tatsumisago, M. *Solid State Ionics* **2004**, *175*, 683–686.
(13) Minami, T; Hayashi, A; Tatsumisago, M *Solid State Ionics* **2006**, *177*, 2715–2720.

Published on Web 09/25/2009

per square centimeter despite the use of highly conducting solid electrolytes.

The interface between the electrode and electrolyte in the all-solid-state batteries differs from that in conventional batteries using liquid electrolytes. Both electrode and electrolyte materials are solid; electrochemical reactions occur through the solid−solid interface between the electrode and solid electrolyte materials. Therefore, formation of a effective electrode−electrolyte interface is important for all-solid-state batteries to achieve high performance.[8] Many studies have been conducted to form an effective electrode−electrolyte interface in all-solid-state batteries.[14−21] Among them, interfacial modification between electrode and solid electrolyte has been an effective technique to improve battery performance, as has been reported for batteries using liquid electrolytes. All-solid-state batteries using $LiCoO_2$ positive electrodes and sulfide solid electrolytes have shown large interfacial resistance between $LiCoO_2$ and solid electrolytes. The interfacial resistances have been decreased greatly through the use of coatings using $LiNbO_3$, $Li_4Ti_5O_{12}$, $LiTaO_3$, and Li_2O-SiO_2 on $LiCoO_2$.[17−21] The reason for the decreased interfacial resistance remains unclear.

Observation and structural analysis of the interface between $LiCoO_2$ and sulfide solid electrolyte is beneficial to reveal the reasons for the large interfacial resistance of the all-solid-state batteries and for the decrease of the interfacial resistance by the coatings. Electrochemical impedance measurements have so far been used mainly to analyze the electrode−electrolyte interface of the all-solid-state batteries using sulfide-based solid electrolytes. On the other hand, transmission electron microscopy (TEM) is a powerful tool to obtain information of the electrode−electrolyte interface. Brazier et al. reported TEM observation of the electrode−electrolyte interface on the thin film batteries using oxide-based solid electrolyte (amorphous $Li_2O-V_2O_5-SiO_2$). Their TEM observations suggested that the deterioration of the interface upon cycling was caused by the migration of the chemical elements between stacked layers.[22] Information about the interface between electrode and electrolyte particles is necessary to construct an ideal electrode−electrolyte interface in all-solid-state batteries. The morphology, structure, and elemental distribution at the interfacial region directly affect the electrochemical performance of the all-solid-state batteries; their investigation enables us to obtain guidelines for the development of all-solid-state batteries with high performance. As described above, it is readily apparent that the interfacial observation between positive electrode and sulfide solid electrolyte is important. Therefore, we have conducted TEM observations of the interface between $LiCoO_2$ and a sulfide solid electrolyte.

In the present work, samples for TEM observation were prepared using a focused ion beam (FIB). The interface between the $LiCoO_2$ electrode and $80Li_2S\cdot20P_2S_5$ glass-ceramic solid electrolyte of all-solid-state cells was studied using TEM and scanning TEM (STEM) with energy dispersive X-ray spectroscopy (EDX). Additionally, we prepared all-solid-state cells using Li_2SiO_3-coated $LiCoO_2$ and compared the electrode−electrolyte interface of the cell using Li_2SiO_3-coated $LiCoO_2$ with that using non-coated $LiCoO_2$ to clarify the coating effect from the perspective of structural changes. Finally, the electrochemical performances of the all-solid-state batteries using noncooated and Li_2SiO_3-coated $LiCoO_2$ were demonstrated. The charge−discharge performance of the all-solid-state batteries using sulfide-based solid electrolytes has been investigated mainly at room temperature to date. As described in this paper, we demonstrate the charge−discharge performance of the batteries in a wide temperature range of −30 to 100 °C. It is difficult for conventional batteries using liquid electrolyte to operate at a temperature of 100 °C because of safety issues; nevertheless, operation at that temperature is beneficial for describing features of all-solid-state batteries.

Experimental Section

1. Preparation of All-Solid-State Cells. The $LiCoO_2$ particles (Toda Kogyo Corp.) used for a positive electrode material were dried at 350 °C before fabricating the all-solid-state cells. The Li_2SiO_3-coated $LiCoO_2$ particles were prepared using the sol−gel method. Lithium ethoxide (LiOEt) and tetraethoxysilane [$Si(OEt)_4$] were diluted to 1 wt % with dry ethanol. Subsequently, the diluted sols were mixed with $LiCoO_2$ particles. After drying at room temperature, the mixture was heated at 350 °C for 30 min. The weight ratio of Li_2SiO_3 coatings to $LiCoO_2$ particles was 0.6 /100. Figures 6−8 show cross-sectional TEM images of 0.6 wt % Li_2SiO_3-coated $LiCoO_2$ particles. The Li_2SiO_3 coating layer on the $LiCoO_2$ particles was confirmed by cross-sectional TEM and SEM-EDX; the thickness was *ca.* 10 nm.[20] More details are described in previous reports.[18,20]

In this study, an $80Li_2S\cdot20P_2S_5$ (mol %) glass ceramic among $Li_2S-P_2S_5$ solid electrolytes was used as a solid electrolyte; the $80Li_2S\cdot20P_2S_5$ glass ceramic is described as a $Li_2S-P_2S_5$ solid electrolyte in this paper. An $80Li_2S\cdot20P_2S_5$ (mol %) glass-ceramic for solid electrolytes was prepared using mechanical milling and subsequent heat treatment.[10] For preparation of the $80Li_2S\cdot20P_2S_5$ glass, Li_2S (99.9%; Idemitsu Kosan Co. Ltd.) and P_2S_5 (99%; Aldrich Chemical Co. Inc.) were used as starting materials. These materials were mechanically milled at 510 rpm for 10 h at room temperature using a planetary ball mill (Pulverisette 7; Fritsch GmbH) with a zirconia pot (45 mL volume) and 160 zirconia balls (5 mm diameter). The obtained

(14) Mizuno, F.; Hayashi, A.; Tadanaga, K.; Tatsumisago, M. *J. Electrochem. Soc.* **2005**, *152*, A1499–A1503.
(15) Hayashi, A; Nishio, Y.; Kitaura, H.; Tatsumisago, M. *Electrochem. Commun.* **2008**, *10*, 1860–1863.
(16) Ohta, N.; Takada, K.; Zhang, L.; Ma, R.; Osada, M.; Sasaki, T. *Adv. Mater.* **2006**, *18*, 2226–2229.
(17) Ohta, N.; Takada, K.; Sakaguchi, I.; Zhang, L.; Ma, R.; Fukuda, K.; Osada, M.; Sasaki, T. *Electrochem. Commun.* **2007**, *9*, 1486–1490.
(18) Sakuda, A.; Kitaura, H.; Hayashi, A.; Tadanaga, K.; Tatsumisago, M. *Electrochem. Solid-State lett.* **2008**, *11*, A1–A3.
(19) Takada, K.; Ohta, N.; Zhang, L.; Fukuda, K.; Sakaguchi, I.; Ma, R.; Osada, M.; Sasaki, T. *Solid State Ionics* **2008**, *179*, 1333–1337.
(20) Sakuda, A.; Kitaura, H.; Hayashi, A.; Tadanaga, K.; Tatsumisago, M. *J. Electrochem. Soc.* **2009**, *156*, A27–A32.
(21) Sakuda, A.; Kitaura, H.; Hayashi, A.; Tadanaga, K.; Tatsumisago, M. *J. Power Sources* **2009**, *189*, 527–530.
(22) Brazier, A.; Dupont, L.; Dantras−Laffont, L.; Kuwata, N.; Kawamura, J.; Tarascon, J-M. *Chem. Mater.* **2008**, *20*, 2352–2359.

glassy powder was heated at 210 °C for 4 h to yield highly conductive $80Li_2S \cdot 20P_2S_5$ glass-ceramic. All-solid-state cells were constructed as follows. The $LiCoO_2$ and the glass-ceramic electrolyte with a weight ratio of 70 : 30 were mixed using an agate mortar to prepare composite positive electrodes. Indium foil (99.999%; Furuuchi Chemical Corp.) was used as a negative electrode. A bilayer pellet consisting of the composite positive electrode (10 mg) and glass-ceramic solid electrolytes (80 mg) was obtained by pressing under 360 MPa (ϕ = 10 mm); indium foil was then attached to the bilayer pellet by pressing under 240 MPa. The pellet was pressed using two stainless steel rods; the stainless steel rods were used as current collectors for both positive and negative electrodes. All the processes for preparation of solid electrolytes and fabrication of all-solid-state batteries were performed in a dry Ar-filled glovebox ([H_2O] < 1 ppm).

2. Electrochemical Measurements. Electrochemical impedance spectroscopy measurements of the all-solid-state cells using noncoated and Li_2SiO_3-coated $LiCoO_2$ were performed using an impedance analyzer (SI 1260; Solartron) after charging them to 3.6 V vs Li−In under 0.13 mA cm^{-2} at room temperature. The applied voltage was 50 mV and the frequency range was from 10 mHz to 1 MHz. The cells were charged and discharged using a charge−discharge measuring device (BTS-2004; Nagano Co. Ltd.). The measurements were conducted at temperatures between −30 and 100 °C. The charge−discharge measurement at 100 °C was conducted at a high current density of 40 mA cm^{-2}.

3. Cross-Sectional Observation of Electrode−Electrolyte Interface. After charging, the layered pellets of $In/80Li_2S \cdot 20P_2S_5/LiCoO_2$ were obtained by removing of stainless steel current collector from the all-solid-state cells. Samples of the $LiCoO_2$/solid electrolyte cross section for TEM observations were obtained using focused ion beam (FIB) milling of the positive electrode layer. The electrode−electrolyte interface was analyzed using TEM (JEM2100F; JEOL). An elemental mapping analysis for the cross-section of the positive electrode layer was conducted using STEM equipped with EDX (JED-2300T; JEOL). The samples were transferred in Ar atmosphere from a globe box to the equipments for FIB and TEM.

Results and Discussion

1. Electrochemical Impedance Spectroscopy on the All-Solid-State Cells Using $LiCoO_2$ Electrode and $Li_2S-P_2S_5$ Solid Electrolytes. Figure 1 shows impedance profiles of the all-solid-state cells using (a, c) noncoated and (b, d) 0.6 wt % Li_2SiO_3-coated $LiCoO_2$. Panels a and b in Figure 1 show impedance profiles of the as-prepared all-solid-state cells with noncoated and 0.6 wt % Li_2SiO_3-coated $LiCoO_2$. No remarkable difference was apparent between the noncoated cell and the cell using Li_2SiO_3-coated $LiCoO_2$ in the impedance profiles before the charge−discharge measurements. Figures 1(c, d) show impedance profiles of the cells after charging to 3.6 V vs Li−In at the current density of 0.13 mA cm^{-2}. Two semicircles are visible in the impedance profiles; their peak top frequencies are about 500 and 1 Hz. The identification of the impedance components has been reported as follows: the resistance observed at the high-frequency region (> 100 kHz) is the resistance of the solid electrolyte layer; the semicircles observed in the medium-frequency (the peak top frequency of about 500 Hz) and

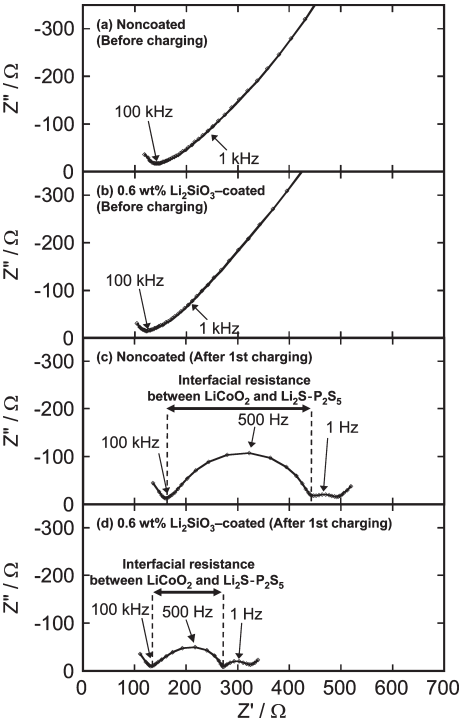

Figure 1. Impedance profiles of the all-solid-state cells $In/Li_2S-P_2S_5$ solid electrolyte/(a,c) noncoated and (b,d) Li_2SiO_3-coated $LiCoO_2$. Measurements were conducted (a, b) before and (c, d) after charging to 3.6 V vs Li−In at the current density of 0.13 mA cm^{-2}.

low-frequency regions (the peak top frequency of about 1 Hz) are, respectively, the resistances in the positive electrode layer (interfacial resistance between $LiCoO_2$ and $Li_2S-P_2S_5$ solid electrolyte) and the negative electrode layer.[20] As presented in Figure 1c, a large interfacial resistance (the resistance observed at 500 Hz) is observed in the cell using noncoated $LiCoO_2$; the resistance decreases because of the Li_2SiO_3-coated $LiCoO_2$. We assume that the large interfacial resistance results from formation of the high-resistance interface between $LiCoO_2$ and sulfide electrolyte.[20]

2. Interfacial Observation between $LiCoO_2$ Electrode and $Li_2S-P_2S_5$ Solid Electrolyte. To obtain information about the interface between $LiCoO_2$ electrode and $Li_2S-P_2S_5$ solid electrolyte, we conducted TEM observations of the positive electrode layer of the all-solid-state cells. The all-solid-state cell using noncoated $LiCoO_2$ after charging to 3.6 V vs Li−In at the current density of 0.13 mA cm^{-2} was used for observations. Figure 2 shows cross-sectional high-angle annular dark field (HAADF) TEM images near the interface between noncoated $LiCoO_2$ and $Li_2S-P_2S_5$ solid electrolyte. Figure 2b shows a magnified image of $LiCoO_2/Li_2S-P_2S_5$ interface presented as a square in Figure 2a. The TEM images show that $LiCoO_2$ electrode and $Li_2S-P_2S_5$ solid electrolyte retains a smooth contact after charging. An interfacial layer is visible at the interface between $LiCoO_2$ electrode and $Li_2S-P_2S_5$ solid electrolyte in Figure 2b. The layer thickness is ca. 10 nm. Figure 3 shows a HAADF−STEM image and EDX mapping for the Co element near the $LiCoO_2$ electrode/$Li_2S-P_2S_5$ solid electrolyte interface. Existence of a Co element of $LiCoO_2$ electrode is observed

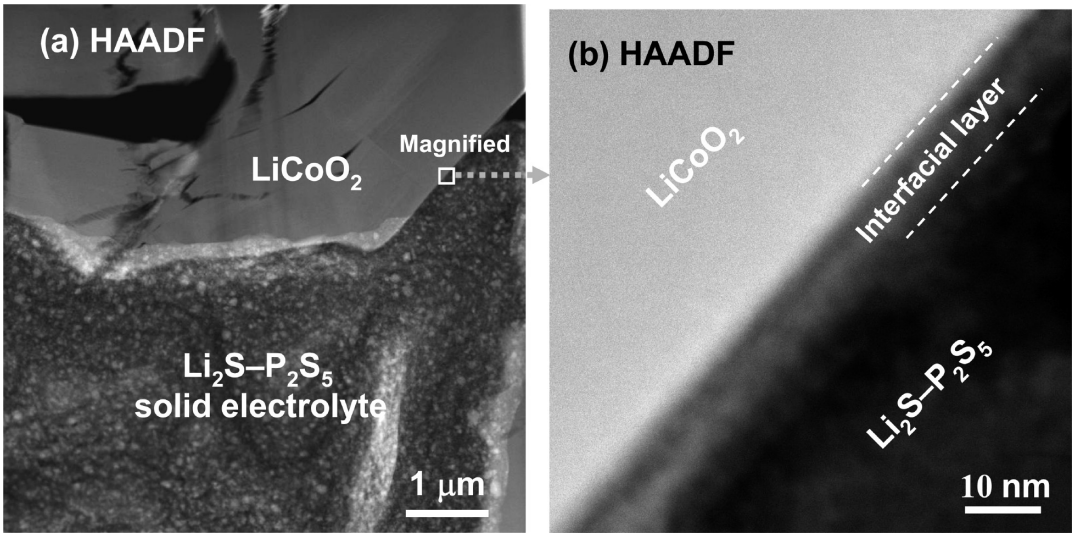

Figure 2. (a) Cross-sectional high-angle annular dark field (HAADF) TEM images of the interface between the $LiCoO_2$ electrode and the $Li_2S-P_2S_5$ solid electrolyte. (b) Magnified image of the area described by the square in a. Observations were conducted after initial charging to 3.6 V vs Li−In.

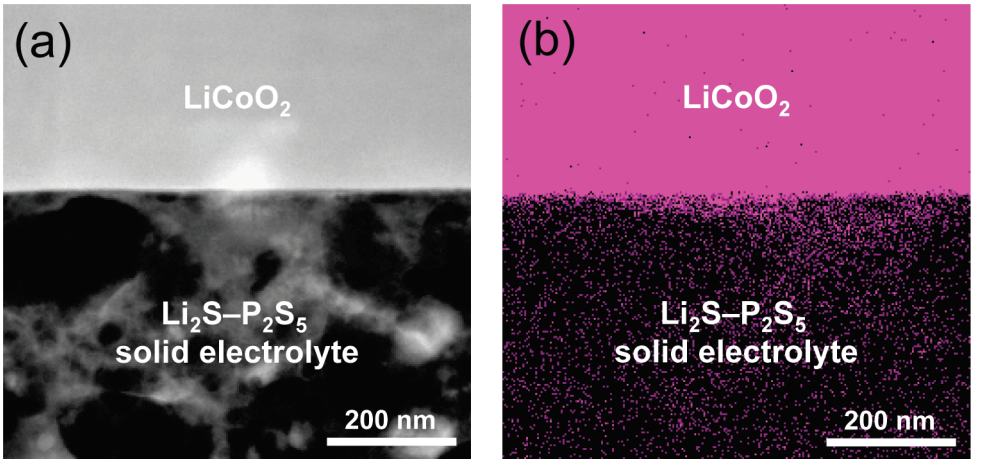

Figure 3. (a) Cross-sectional HAADF−STEM image and (b) the corresponding EDX mapping for the Co element near the $LiCoO_2$ electrode/$Li_2S-P_2S_5$ solid electrolyte interface after initial charging.

in $Li_2S-P_2S_5$ solid electrolyte, indicating Co diffusion from $LiCoO_2$ to $Li_2S-P_2S_5$. More details are available from EDX line profiles at the region near the $LiCoO_2$ electrode/$Li_2S-P_2S_5$ solid electrolyte interface. Figure 4a shows the HAADF−STEM image of the $LiCoO_2$/$Li_2S-P_2S_5$ interface. Figure 4b presents the EDX line profiles of the existence ratio for Co, S, and P elements at the position indicated by the arrow in Figure 4a. The coexistence of Co, S, and P elements is observed at the interfacial layer, indicating that the elements of $LiCoO_2$ and $Li_2S-P_2S_5$ solid electrolyte mutually diffuse. In particular, the Co diffusion from $LiCoO_2$ to $Li_2S-P_2S_5$ is outstanding; the Co element is observed even at a distance of 50 nm from the interface. Moreover, the EDX line profile shows small S diffusion into $LiCoO_2$. The mutual diffusion of Co, S, and P is related to the formation of the interfacial layer. The interfacial region nanostructure is observed using nanoarea electron diffraction (n-ED), which selectively analyzes the interfacial materials. Figure 5 presents a cross-sectional HAADF−STEM image and the n-ED pattern of the $Li_2S-P_2S_5$ solid electrolyte, interfacial layer, and $LiCoO_2$ electrode. The n-ED pattern of the solid electrolyte (position 1) shows that the solid electrolyte is amorphous. The n-ED patterns of $LiCoO_2$ electrode show the same diffraction patterns from inside to the surface (position 4 and 5), indicating that the $LiCoO_2$ is a single crystal and that large degradation does not occur. On the other hand, the n-ED patterns of the interface layer (position 2 and 3) show patterns suggesting the presence of a nanosize polycrystal. The EDX analysis shows that the interfacial layer mainly comprises Co and S. Uchimoto et al. reported from X-ray absorption spectroscopy that a compound whose electronic state resembles that of CoS is produced at the interface between $LiCoO_2$ and sulfide electrolyte during charge−discharge cycling.[23] Consequently, it is assumed that nanosize polycrystalline cobalt sulfides exist at the interfacial layer. However, identification of the polycrystals is difficult because there are no remarkable spots in the n-ED pattern. Further analyses are

(23) Uchimoto, Y.; Wakihara, M. In *Solid State Ionics for Batteries*; Minami, T. Ed.; Springer-Verlag: Tokyo, 2005; p 126.

necessary to clarify the interfacial structure in greater detail.

The interfacial TEM observation revealed that the interfacial layer was formed at the interface between $LiCoO_2$ and $Li_2S-P_2S_5$ solid electrolyte. Moreover, mutual diffusion of Co, P, and S was observed at the interface. The formation of the interfacial layer and the mutual diffusion indicates the degradation of the $LiCoO_2$ electrode and $Li_2S-P_2S_5$ solid electrolyte near the interface. Degradation of the interface is inferred as one cause of the large interfacial resistance of the electrode−electrolyte interface of the all-solid-state batteries using $LiCoO_2$ electrode and $Li_2S-P_2S_5$ solid electrolytes. Suppression of both the formation of the interfacial layer and the diffusion is expected to be effective in decreasing the interfacial resistance and bringing about improvement of the electrochemical performance of all-solid-state cells.

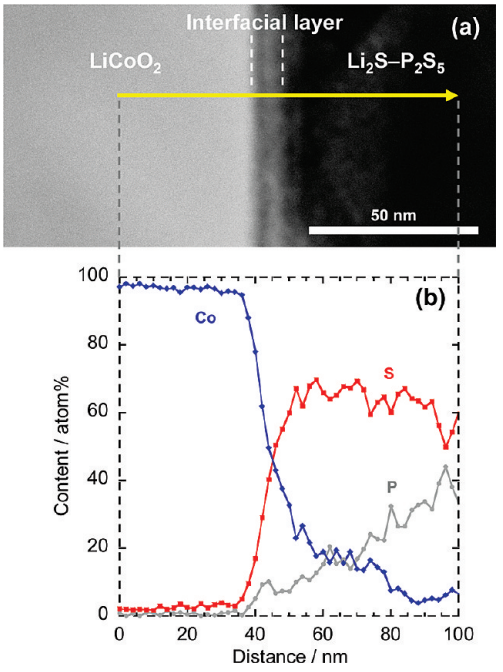

Figure 4. (a) Cross-sectional HAADF−STEM image of $LiCoO_2$ electrode/$Li_2S-P_2S_5$ solid electrolyte interface after initial charging and (b) cross-sectional EDX line profiles for Co, P, and S elements. The arrow in a presents the positions at which EDX measurements were taken.

3. Interfacial Observation between Li_2SiO_3-Coated $LiCoO_2$ Electrode and $Li_2S-P_2S_5$ Solid Electrolyte. Here, it has been revealed that the interfacial layer was formed and that the elements of Co, P, and S mutually diffused at the interface between $LiCoO_2$ and the $Li_2S-P_2S_5$ solid electrolyte. These results suggest interfacial structural changes, which would cause the high interfacial resistance for lithium-ion conduction between $LiCoO_2$ and solid electrolyte. Oxide coatings have been reported as an effective means to decrease the interfacial resistance of the all-solid-state cells using sulfide solid electrolyte, as presented in Figure 1. In this section, we specifically examine the electrode−solid electrolyte interface of the cell using Li_2SiO_3-coated $LiCoO_2$ particles as a positive electrode material. The Li_2SiO_3 coating is effective in decreasing the interfacial resistance (Figure 1) and improving the high rate performance of the all-solid-state cells using $LiCoO_2$ electrode and $Li_2S-P_2S_5$ solid electrolyte.[18,20] We specifically investigated the $LiCoO_2/Li_2S-P_2S_5$ interface of the

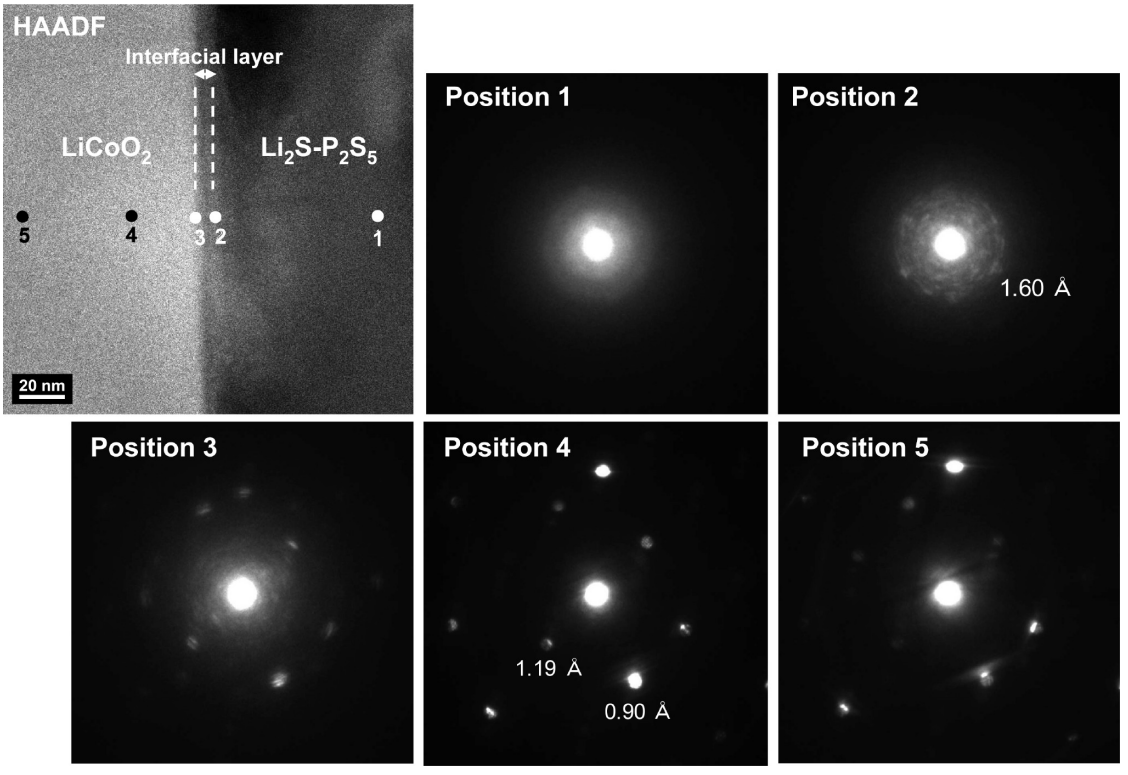

Figure 5. Cross-sectional HAADF−STEM image and the n-ED patterns of the $Li_2S-P_2S_5$ solid electrolyte, the interfacial layer, and the $LiCoO_2$ electrode after initial charging. The numbered points in the HAADF-STEM image correspond to the positions of n-ED measurements.

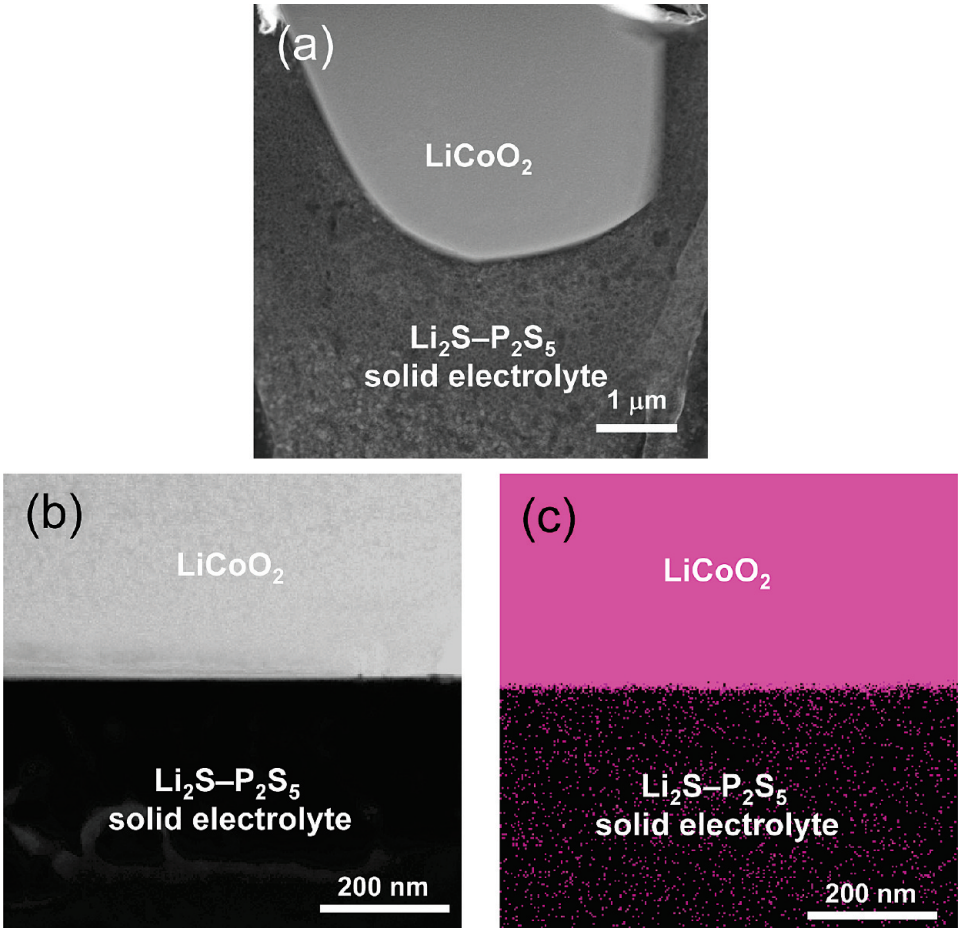

Figure 6. (a) Cross-sectional HAADF−STEM image near the Li_2SiO_3-coated $LiCoO_2$ electrode/$Li_2S-P_2S_5$ solid electrolyte interface after initial charging. (b) Magnified image of cross-sectional HAADF-STEM image. (c) EDX mapping for the Co element in the area corresponding to b.

cell using Li_2SiO_3-coated $LiCoO_2$ after charging to 3.6 V vs Li−In.

Images a and b in Figure 6 show the HAADF−STEM image and (c) the EDX mapping for Co element near the Li_2SiO_3-coated $LiCoO_2$ electrode/$Li_2S-P_2S_5$ solid electrolyte interface. The $LiCoO_2$ and $Li_2S-P_2S_5$ solid electrolyte retain their smooth contact (Figure 6a). The EDX mapping shows that the Co diffusion from $LiCoO_2$ to $Li_2S-P_2S_5$ is suppressed by Li_2SiO_3 coatings. Figure 7a shows the HAADF−STEM image; Figure 7b shows EDX line profiles of the existence ratio for Co, P, S, and Si elements at the position indicated by the arrow in Figure 7a. In the STEM image, the interfacial layer is visible. The EDX line profile shows that the Si element of the Li_2SiO_3 coating is visible at the interface. The EDX line profile also shows coexistence of Co, P, and S elements at the interfacial region. The Co diffusion is observed between about 30 nm. Figure 8 presents the cross-sectional HAADF−STEM image and the n-ED patterns of the interface between Li_2SiO_3-coated $LiCoO_2$ electrode and $Li_2S-P_2S_5$ solid electrolyte. The n-ED pattern of $Li_2S-P_2S_5$ solid electrolyte (position 5) shows that the solid electrolyte is amorphous. The n-ED pattern of the interfacial layer (position 4) shows that the interfacial layer is amorphous. The n-ED patterns of $LiCoO_2$ (positions 1−3) show the same patterns, indicating that

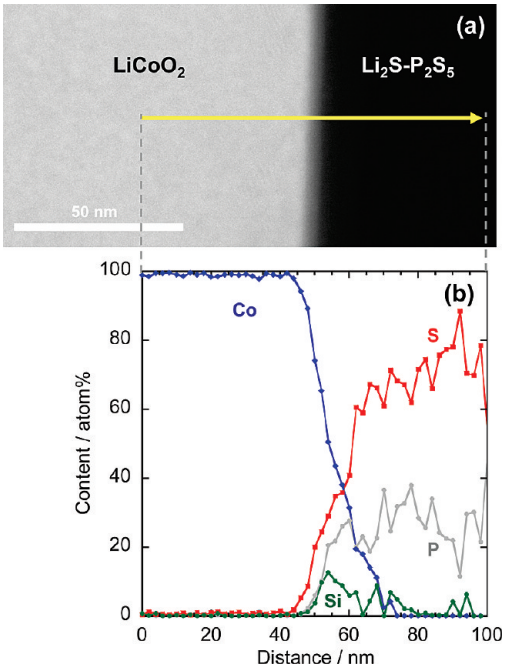

Figure 7. (a) Cross-sectional HAADF−STEM image of the Li_2SiO_3-coated $LiCoO_2/Li_2S-P_2S_5$ interface after initial charging and (b) cross-sectional EDX line profiles for Co, P, S, and Si elements. The arrow in a indicates the positions of the EDX measurements.

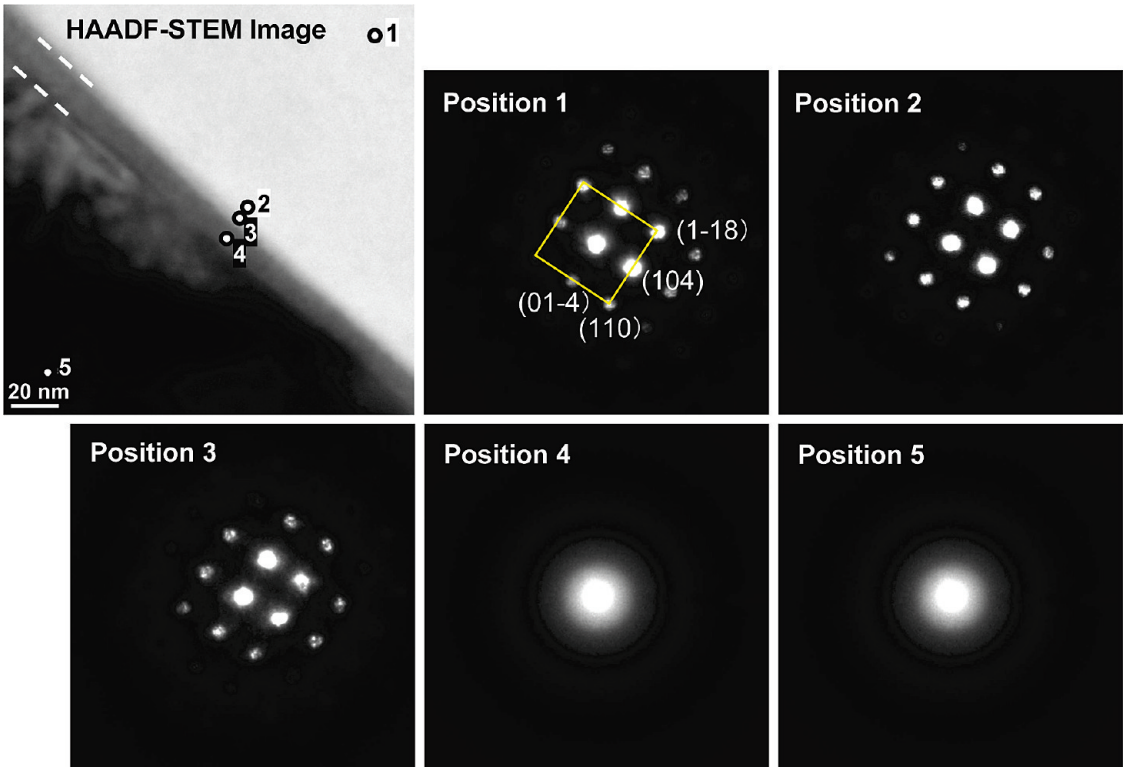

Figure 8. Cross-sectional HAADF−STEM image and the n-ED patterns of the interface between Li_2SiO_3-coated $LiCoO_2$ electrode and $Li_2S-P_2S_5$ solid electrolyte after initial charging. The numbered points in the HAADF−STEM image correspond to the positions of n-ED measurements.

the $LiCoO_2$ particle is single-crystal and that large degradation does not occur. The Co and S exist at the interfacial layer also in the presence of Li_2SiO_3 thin films; cobalt sulfides would form partially at the interfacial layer. However, the Co diffusion at the interface in the presence of the Li_2SiO_3 thin film decreases compared to that at the interface without Li_2SiO_3 thin film (Figures 3 and 4). The Co diffusion is suppressed by the Li_2SiO_3 coating layer. The Li_2SiO_3 acts as a buffer layer preventing Co diffusion from the $LiCoO_2$ electrode to $Li_2S-P_2S_5$ solid electrolyte. Nanocrystalline materials are not observed in the n-ED patterns when using Li_2SiO_3-coated $LiCoO_2$. The interfacial layer in this case is considered as an amorphous Li_2SiO_3 coating layer. The Li_2SiO_3 coatings suppress formation of the polycrystalline interfacial products. The interfacial Li_2SiO_3 coating is effective in preventing the direct contact between $LiCoO_2$ and $Li_2S-P_2S_5$ and suppressing degradation of the interface such as the mutual elemental diffusion and the interfacial layer formation.

Ohta et al. proposed a "space−charge layer model" to explain the large interfacial resistance between $LiCoO_2$ and the sulfide solid electrolytes in all-solid-state batteries using $Li_{3.25}Ge_{0.25}P_{0.75}S_4$ (thio−LISICON) as a solid electrolyte.[16,17,19] In the model, the reason for the large interfacial resistance is considered to be formation of a lithium-deficient layer (space−charge layer) at the interface. The space−charge layer results from lithium-ion transfer from the sulfide electrolyte to $LiCoO_2$ because of the large difference in electrochemical potentials in these materials. The coatings of $Li_4Ti_5O_{12}$, $LiNbO_3$, and $LiTaO_3$ on the $LiCoO_2$ electrode yielded a low interfacial resistance in the all-solid-state batteries, and Ohta et al. suggested that the oxide coatings act as a buffer layer to suppress the formation of the space−charge layer.[16,17,19]

In this study, we identified structural changes caused by the diffusion of Co, P, and S elements and the formation of new interfacial layers mainly composed of Co and S at the $LiCoO_2/Li_2S-P_2S_5$ interface. These phenomena are one reason for the large interfacial resistance of the all-solid-state batteries. The coating of Li_2SiO_3 on $LiCoO_2$ was effective in suppressing the interfacial layers. We thus believe that the suppression of the interfacial layers is the main reason for the reduction of interfacial resistance between $LiCoO_2$ electrode and $Li_2S-P_2S_5$ solid electrolyte.

4. Electrochemical Performance of the All-Solid-State Cells Using $LiCoO_2$ Electrode and $Li_2S-P_2S_5$ Solid Electrolyte. All-solid-state batteries using Li_2SiO_3-coated $LiCoO_2$ particles reportedly show good electrochemical performance at room temperature.[18,20] We demonstrate herein the all-solid-state batteries using $LiCoO_2$ electrode and $Li_2S-P_2S_5$ solid electrolytes at extremely low and high temperatures.

Panels a and b in Figure 9 show impedance profiles of the all-solid-state cells using noncoated and Li_2SiO_3-coated $LiCoO_2$ at −30 °C after charging to 3.6 V vs Li−In, which corresponds to 4.2 V vs Li. The internal resistance of the cells at the low temperature of −30 °C is much larger than that at room temperature, as presented in Figure 1. The resistances attributed to a solid electrolyte layer (the

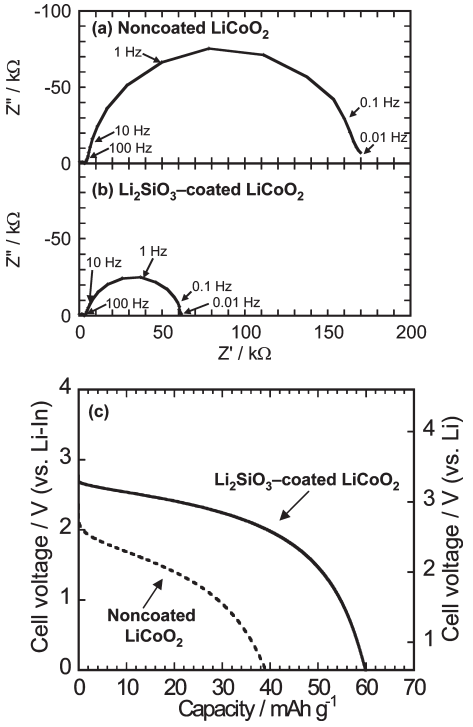

Figure 9. Impedance profiles of the all-solid-state cells In/$Li_2S-P_2S_5$ solid electrolyte/(a) noncoated and (b) Li_2SiO_3-coated $LiCoO_2$ at −30 °C after charging to 3.6 V vs Li−In. (c) Discharge curves of the all-solid-state cells under the current density of 0.064 mA cm^{-2} at 30 °C.

resistance observed more than 100 Hz) are ca. 3000 Ω in each cell. The interfacial resistances between $LiCoO_2$ and solid electrolytes (the large semicircles) are, respectively, 1.6×10^5 Ω (a) and 6.0×10^4 Ω (b). The interfacial resistance of the cell using Li_2SiO_3-coated $LiCoO_2$ is about one-third of that of a cell using noncoated $LiCoO_2$. Figure 9c presents discharge curves of the all-solid-state cells under the current density of 0.064 mA cm^{-2} at −30 °C. The all-solid-state cells are discharged even at the low temperature of −30 °C. The discharge capacity of the cell using the Li_2SiO_3-coated $LiCoO_2$ is 60 mA h g^{-1}, although that of the noncoated $LiCoO_2$ is less than 40 mA h g^{-1}. The decrease in the interfacial resistance by oxide coating contributes to a high voltage plateau and large discharge capacity.

The all-solid-state batteries are expected to function even under high temperatures at which conventional batteries function poorly. Figure 10 presents the charge−discharge performance of the all-solid-state cells using $LiCoO_2$ coated with Li_2SiO_3 at 100 °C under the current density of 40 mA cm^{-2}. All-solid-state cells function even under the high temperature of 100 °C. Moreover, the all-solid-state cell using Li_2SiO_3-coated $LiCoO_2$ works at an extremely high current density of 40 mA cm^{-2}, which corresponds to 40 C; the charge−discharge capacity is

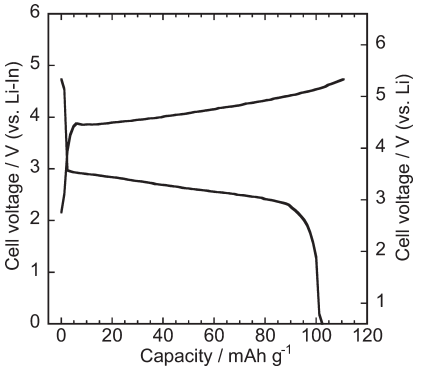

Figure 10. Charge−discharge curves of the all-solid-state cell In/$Li_2S-P_2S_5$ solid electrolyte/Li_2SiO_3-coated $LiCoO_2$ at 100 °C under the current density of 40 mA cm^{-2}.

more than 100 mAh g^{-1}. Although the diffusion at the interface at the high temperature of 100 °C probably accelerate compared to that at 25 °C, the Li_2SiO_3 coatings act as a buffer layer to suppress the side reaction at the interface such as the mutual diffusion of Co, P, and S.

Conclusions

The interface between $LiCoO_2$ electrode and $Li_2S-P_2S_5$ solid electrolyte in the all-solid-state batteries was observed using TEM and STEM. The interfacial layer formed after charging the batteries was observed between the electrode and the solid electrolytes by TEM. Moreover, Co, P, and S elements mutually diffused between $LiCoO_2$ and the $Li_2S-P_2S_5$ solid electrolyte. These results reflected that side reactions occurred at the electrode−electrolyte interface. Those phenomena at the interface were suppressed using Li_2SiO_3 coatings, which caused lower interfacial resistance between $LiCoO_2$ and $Li_2S-P_2S_5$ solid electrolyte. Results showed that suppression of the formation of the interfacial layer was effective in improving the electrochemical performance of the all-solid-state batteries. The all-solid-state cells functioned even at the low temperature of −30 °C. Moreover, the all-solid-state cell using Li_2SiO_3-coated $LiCoO_2$ was charged and discharged under a significantly high current density of 40 mA cm^{-2}.

Designing an effective electrode−electrolyte interface is important to achieve good battery performance, especially with respect to all-solid-state batteries; interfacial observation using TEM is a useful technique to ascertain guidelines for designing an ideal electrode−electrolyte interface.

Acknowledgment. A Grant-in-Aid for Scientific Research from the Ministry of Education, Culture, Sports, Science and Technology of Japan supported this work. The New Energy and Industrial Technology Development Organization (NEDO) of Japan also supported this study.